Egypt.J.Chem. **Vol. 63**, No.5. pp. 1679 - 1696 (2020)

Egyptian Journal of Chemistry
http://ejchem.journals.ekb.eg/

Chemical Functionalization Graphene Oxide for The Adsorption Behavior of Bismarck Brown Dye from Aqueous Solutions

Alaa A. Mizhir[1], Ali A. Abdulwahid[2] and Hadi S. Al-Lami*[2]
[1]*Department of Applied Marine Science, Faculty of Marine Science, University of Basrah, Basrah, Iraq*
[2]*Department of Chemistry, College of Science, University of Basrah, Basrah, Iraq*

THE adsorption behavior of cationic dye Bismarck brown BB onto graphene oxide GO, graphene oxide derivatives 3,3′-Diaminobenzidine GODAB, and Ethylene diamine tetraacetic acid-modified graphene oxide GODABE as adsorbents from aqueous solutions were investigated, and characterized by various techniques, like Fourier transform infrared spectroscopy, Field Emission Scanning Electron Microscopy, and X-ray diffraction spectroscopy. Adsorption of BB dye on modified graphene oxide was explored in a series of batch experiments under various conditions. The data were analyzed using Langmuir and Freundlich, models. The Langmuir model was found to be more suitable for the experimental data than other adsorption models. The maximum adsorption capacities were 714.28, 1428.5, and 1111.1 mg/g for GO, GODAB, and GODABE at optimum pH 3 for GO and GODAB, 5 for GODABE and the optimum agitation time were chosen as 45min for GO and 30min for both adsorbents GODAB and GODABE. Kinetic studies revealed that the pseudo-second-order model showed the best fitting to the experimental data. The thermodynamic parameters imply that the adsorption process was spontaneous and endothermic.

Keywords: Adsorption isotherm, Bismarck Brown BB, Graphene Oxide, Pseudo-second-order model.

Introduction

The disposal of textile wastewater is currently a major problem from a global viewpoint. Textile industries produce a lot of wastewater, which contains several contaminants, including acidic or caustic dissolved solids, toxic compounds, and dyes [1]. Among textile effluents, synthetic dyes are hardly eliminated under aerobic conditions and are probably decomposed into carcinogenic aromatic amines under anaerobic conditions [2]. Besides, it is difficult to remove reactive dyes using chemical coagulation due to the dyes' high solubility in water [3]. Synthetic dyes are commonly used in many industries such as textile, leather, tanning, paper, rubber, plastics, cosmetics, pharmaceutical and food industries. Synthetic dyes, classified by their chromophores, have different stable chemical structures and are not often degraded or removed by conventional physical and chemical processes [4,5]. Bismarck Brown is a cationic basic diazo dye. It is used in color paper, pulp, wool, and leather, etc. materials both, short time and prolonged contacts of the dye with the eye and skin causes severe irritation with redness at the site of contact [6]. It is poisonous to aquatic organisms. It should not release into a culvert or waterways. Adsorption is a simple, economic and promising technique for sewage refinement, which has the attributes of high selectivity and design ability [7]. Adsorbent assumes a key role in the adsorption process. In this way, the design and synthesis of the adsorbents with execution adsorption performance are a significant subject in adsorption research [8]. Graphene oxide, GO, is a built nanomaterial that comprises of different functional groups, including hydroxyl, carboxyl, and epoxy groups. These groups can't just

*Corresponding author e-mail: hadi.abbas@uobasrah.edu.iq
Received 21/12/2019; Accepted 3/2/2020
DOI: 10.21608/ejchem.2020.21260.2271

upgrade the dispensability of GO but also serve as adsorption destinations for different contaminants in aqueous solution [9,10]. Ethylene diamine tetraacetic acid EDTA is a decent coordination agent with six ligands. Up until this point, EDTA has been broadly applied in dyeing assistants [11]. Such an expansive utilization of EDTA is because of that it could form coordination complexes with most metal ions and dyes. In light of this principle, EDTA would be a good candidate for adsorbent and could be used for removal of metal ions, and its composition with different materials for the pollutant evacuation is critical and attainable [12]. The point of this paper is to assess the adsorption capability of GO modified with DAB and EDTA for the removal of BB dye from aqueous solutions.

Experimental

Materials and Instruments

All chemicals are of reagent grades and purchased from Sigma-Aldrich Company. They were used without any further purification.

Fourier-transform infrared FTIR spectra of compounds were analyzed using a FTIR-8101M Shimadzu spectrometer as KBr discs in the region 400-4000 cm^{-1} to investigate the chemical structures. Morphology of the prepared materials was identified using an Emission Scanning Electron Microscope (FESEM) type FEI NOVA Nano SEM 450 under vacuum at an operating voltage of 10 kV. Patterns of X-ray diffraction (XRD) of the adsorbents were recorded by a Rigaku X-ray Powder Diffractometer (Japan) at a scanning speed of 2 min^{-1} from 5 to 80° (Cu K_α radiation with a wavelength of 1.5406 Å). The concentration of BB dye was measured in a quartz cell of 1cm length at λ_{max} 457 nm using a Sentry 20 UV-Visible spectrophotometer model T180.

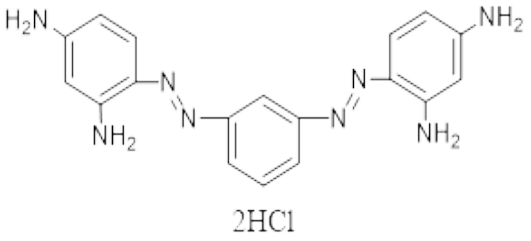

Fig. 1. Chemical structure of Bismarck Brown (BB).

Methods

Synthesis of graphene oxide (GO)

GO was prepared through a modified Hummers method [13]. 2.0 g graphite powder and 1.0 g $NaNO_3$ were dissolved in 46.0 mL H_2SO_4 (98%) under an ice bath. After stirring for 15 min, 6.0g $KMnO_4$ was gradually added to the suspension with slowly stirring as possible to control the temperature below 20°C. The suspension was stirred for 2 h with maintaining at 35°C for 30 min. 100.0 mL deionized water was poured to the suspension, resulting in a quick increase in temperature, and the temperature should be controlled lower than 98°C. After 15 min, the suspension was then further diluted to 280.0 mL with warm deionized water. 20.0 mL H_2O_2 (30%) was added, and change the suspension color to luminous yellow. Then, the suspension was filtered and washed a warm aqueous solution of 5% HCl and deionized water, respectively, until no sulfates were detected, and the pH of the filtrate was adjusted to 7.0. The graphene oxide GO was dried under vacuum at 50°C.

Synthesis of functionalized graphene oxide (GODAB and GOBABEDTA)

To synthesize 3,3′-Diaminobenzidine-functioned graphene oxide [14], 0.5 g GO was ultrasonically dispersed in 10.0 mL distilled water for 5 min at room temperature followed by adding a mixture of 2.5 g Sodium hydroxide NaOH and 2.5g Sodium chloroacetate $ClCH_2COONa$, then the suspension was slowly stirred and ultrasonically treated at room temperature for 2h to convert hydroxyl and epoxide groups in GO to carboxylic groups.

The resulting product, carboxylic graphene oxide GOCOOH, was neutralized by dilute hydrochloric acid and dried under vacuum at 80°C for 24h. A mixture of 5.0mL thionyl chloride and 25.0 mL DMF was added to 0.5g GOCOOH and refluxed at 70°C for 24 h. The resulting product, acyl chloride graphene oxide GOCOCl, was centrifuged for 8 min at 5000 RPM and thoroughly washed with tetrahydrofuran THF several times and dried in an oven at 80°C. 2.0 g 3,3′-Diaminobenzidine (DAB) was added to GOCOCl and ultrasonically treated for 2h at room temperature. Afterwards, the suspension was refluxed at 110°C for 24h to carry out the reaction. GODAB was cooled and washed with ethanol to remove any excess of DAB, and finally dried in vacuum for 24h.

For the preparation of GODAB-functioned ethylenediaminetetraacetic acid (GODABE), 1.0 g GODAB was dispersed in 20.0mL 10% acetic acid to form GODAB dispersion, 6.0 g ethylenediaminetetraacetic acid (EDTA) was evenly dispersed in 100.0 mL methanol to get

EDTA dispersion. Then GODAB and EDTA dispersions were mixed by mechanical stirring and react at room temperature for 24h. The obtained product GODABE was filtered, washed twice with ultrapure water, dried at 50°C, and ground into a fine powder [15].

Batch experiments

Batch adsorption experiments of Bismarck Brown dye were carried out to evaluate the adsorption parameters and factors influencing adsorption, the numbers of adsorbents GO, GODAB, and GODABE were kept at 0.025 g which placed into 400.0 mg/L solution of BB dye for all adsorbents, and the volume of dye was 0.1 L. The adsorption experiments were conducted on a thermostat shaker at 27°C and shaking at 200rpm for a particular period time. After adsorption, adsorbents separated from the solution by centrifugation, and the concentration of the remaining BB dye was determined with a UV-T180 spectrophotometer at λ_{max}.

Adsorption processes were carried out at optimum conditions applying agitation time (3, 9, 12, 15, 30, 45, and 60 min), at pH of the BB dye equal 3.0 for GO and GODAB, 5.0 for GODABE. The amount of the dye on the adsorbents was evaluated to the following equation, Eq. 1:

$$q_e = \frac{(C_o - C_2)V}{m} \quad \ldots\ldots\ldots (1)$$

Where C_o and C_e (mg/L) are the initial and the equilibrium concentrations of BB dye in the solution, V (L) is the volume of the BB dye solution, m (g) is the mass of the used adsorbents and q_e (mg/g) is the amount of adsorbed BB dye per gram of adsorbents GO, GODAB, and GODABE (adsorption capacity).

Desorption studies

Desorption of dye from adsorbents was carried out by applying three times adsorption/desorption experiments using the same adsorbents, maximum adsorption of dye conducted by applying optimum agitation time, and pH-value for each adsorbent in this work. The desorption experiments were done by immersing dye-loaded adsorbent into (1.0M) $NaClO_4$ solution, and the mixture was stirred continuously for 60min at room temperature, and the desorbed dye was separated by centrifugation and filtration, then the concentration of dye determined spectrophotometrically as mention before [16]. The efficiency of removal (S) was determined by Eq. 2:

$$S = \frac{(C_d - V_d)}{(q_e \,.\, W)} \; x100\% \quad \ldots\ldots\ldots (2)$$

Where (S) is an efficiency of dye desorption, (C_d) is the concentration of dye in solution after desorption, (V_d) is the eluent volume.

Adsorption isotherms

The analysis of the adsorption isotherm data by fitting them to different isotherm models is a significant advance to find a reasonable model [2,11] that can be used for design purposes. In our study, the two Langmuir and Freundlich models were utilized to look at the relationship between the adsorbed dye amount and its equilibrium concentration [17]. The linear forms of Langmuir and Freundlich isotherms are given in Eqs. 3 and 4 respectively:

$$\frac{C_e}{q_e} = \frac{1}{q_m \,.\, K_L} + \frac{C_e}{q_m} \quad \ldots\ldots\ldots (3)$$

$$\ln q_e = \ln K_F + \frac{1}{n} \ln C_e \quad \ldots\ldots\ldots (4)$$

Where C_e the dye equilibrium concentration; K_L the Langmuir constant that relates to the energy of adsorption; K_F the Freundlich constant related to the adsorption capacity; 1/n the adsorption intensity; q_m the adsorbent monolayer capacity. The essential characteristics of a Langmuir isotherm can be expressed in terms of dimensionless constant separation factor or equilibrium parameter R_L which is defined by:

$$R_L = \frac{1}{(1 + K_L . C_e)} \quad \ldots\ldots\ldots (5)$$

R_L is indicative of the isotherm shape and predicts whether a sorption system to be either favorable ($0<R_L<1$), unfavorable ($R_L>1$) or irreversible ($R_L=0$) [18].

Kinetic assessment

Kinetics data help to depict dye uptake rates, which control the residence time of adsorbate at the solid-liquid interface and give helpful information for adsorption process designing [9]. Experimental kinetic curves can be assessed using various models [2,10]. In our study, the appropriateness of pseudo-first-order, pseudo-

$$\frac{1}{q_t} = \frac{K_1}{(q_1 \,.\, t) + \frac{1}{q_1}} \quad \ldots\ldots\ldots (6)$$

$$\frac{t}{q_t} = \frac{1}{(K_2 \cdot q_2^2) + \frac{1}{q_2} \cdot t} \quad \ldots\ldots\ldots (7)$$

$$q_t = (K_p \cdot t^{\frac{1}{2}}) + C \quad \ldots\ldots\ldots (8)$$

second-order, and Intra-particle diffusion models were tested to interpret the mechanism of BB dye adsorption onto GO, GODAB, and GODABE. The linear form of the three kinetic model equations can be expressed as follow:

Where q_t and $q_{(1+2)}$ are the amounts of adsorbed dye at time t, and equilibrium respectively; K_1 is the adsorption rate constant of pseudo-first-order model; K_2 is the adsorption rate constant of pseudo-second-order model; K_p is the adsorption rate constant of the intra-particle diffusion model; C is the constant, which gives a thought regarding the boundary layer thickness.

Adsorption thermodynamics

Thermodynamic parameters can be determined from the thermodynamic equilibrium constant, K_L (or the thermodynamic distribution coefficient), whereas K_L equal to:

$$K_L = \frac{C_a}{C_e}$$

Where C_a (mg/g) and C_e (g/L) is the adsorbed and the remaining CR dye respectively. The results of thermodynamic studies make it conceivable to understand the feasibility of the adsorption process and to get helpful data about fundamental parameters of adsorption, such as the change of the standard enthalpy (ΔH°), the change of standard entropy (ΔS°), and the change of standard free energy (ΔG°); that can be calculated by Eqs. 9 and 10:

$$\ln K_L = \frac{\Delta S^o}{R} - \frac{\Delta H^o}{RT} \quad \ldots\ldots\ldots (9)$$

$$\Delta G^o = \Delta H^o + T\Delta S^o \quad \ldots\ldots\ldots (10)$$

Where R is the universal gas constant (8.314 J/mol K), and T is the absolute temperature.

Results and Discussion

Characterization of adsorbents

Fourier-transforms infrared spectrometry (FTIR)

The presence of the additional functional groups on the modified graphene oxide (GO) surface was studied using FTIR spectroscopy. The spectrum of layer graphite powder is nearly featureless, while that of GO exhibit prominent bands at 3367 cm^{-1}, corresponds to hydroxyl stretching vibration, and at 1728 cm^{-1} corresponding to the stretching vibration of the carbonyl group. While the peak at 1620cm^{-1} was attributed to aromatic C=C stretching vibrations. The FTIR spectra of GO and graphite were significantly different, where a high amount of oxygen-containing functional groups are present in the basal and edge planes of graphene oxide sheet [19], and the differences were generally proportionate to those that have been described beforehand [20], indicating that we successfully prepared the graphene oxide.

Successful amidation reaction between DAB amine groups and carboxylic acid sites of GO was confirmed FTIR spectroscopy. The nature of the interaction between GO and DAB is confirmed by the appearance of the peaks at 1607 cm^{-1} (C=O stretching of amide group), 1565 cm^{-1} (N-H bending of amide group), 1062 cm^{-1} (C-N stretching) and intense peak at 1027cm^{-1} (N-H wagging vibration of amine group) along with a broadband at 3417 cm^{-1} (N-H stretching). This indicated the successful formation of amide linkages as well as the occurrence of nucleophilic substitution reactions, as proposed in the reaction mechanism. The important absorbance peaks of the GODABE around 1080 cm^{-1} were caused by the stretching and bending vibrations of the N–H bond [21]. The broadband around 3423 cm^{-1} might ascribe to the O–H stretching vibration from adsorbed H_2O on the surface of GODABE and GO components [22]. The band at 1635 cm^{-1} was attributed to the vibration of the C=O bond originating from carboxyl functional groups. Besides, C–OH vibration at 1410 cm^{-1} and C–H saturated bond at 3017 cm^{-1} were observed in GODABE [20]. Besides, the C-O stretching vibration peak shifts from 1607 cm^{-1} (GODAB) to 1686 cm^{-1} (GODABE) [23], indicating interactions exist between GODAB and EDTA. The FTIR confirmed that the prepared GODAB and GODABE contained plentiful oxygen and nitrogen functional groups, all the functional groups could act as available adsorption sites and played an important role in the adsorption process. A new strong peak at 1202 cm^{-1} was due to the C-O stretching vibration of new COO^- groups from EDTA. The strong new broadband of 1317 cm^{-1} in GODABE was attributed to the COO^- symmetric and asymmetric stretching vibrations [24].

Field emission scanning electron microscopy (FESEM)

The grain size and surface morphology were observed and investigated through field emission scanning electron microscope FESEM. According to Fig. 2 (a, b and c), GO is seen as a flat sheet with some pucker on the surface which is due to deformation of graphite upon the exfoliation by potassium permanganate the strong oxidizing agent (Fig. 2a), and have well defined and interlinked three-dimensional Graphene sheets, forming a porous network that resembles a loose sponge. Fig. 2b shows the FESEM image of GODAB, that appearance as quite different compared to GO, and reveals that it is a porous structure with a large number of adsorption sites, and also observed that the surface of GO sheet is smooth and tightly packed owing to the interactions of oxygen functional groups [25]. It indicates and confirms the combination of graphene oxide and the amine compound. Furthermore, as seen in Fig. 2c, the cross-section of GODABE shows a surface morphology that is quite different from that of GO or GODAB. While there are obvious wrinkles on GODABE surface, that is much smoother than either GO or GODAB.

X-ray powder diffraction (XRD)

The XRD patterns of GO, GODAB, and GODABE are shown in Fig. 3 (a, b and c). the XRD of the graphite layer has a sharp diffraction peak at 2θ (26.25°), corresponding to an interlayer distance of (0.34 nm), which is following the reported value [26]. As Fig. 3a, the GO powder sheet shows a sharp peak at 2θ position (~9.55°), which corresponds to an interlayer distance of (0.924 nm). The enlarged interlayer distance is attributed to the presence of oxygen functional groups on the GO sheet and suggests the successful oxidation process of the graphite layer [27]. Meanwhile, after functionalization of GO with DAB, many new peaks have appeared (Fig. 3b), the most important of those peaks are centered at 2θ (17.3°, 31.6°, 37.8°, and around 45.0°). In the GO-functioned with DAB, we observed weak peaks appearing nearly at 2θ (7.7° and 9.0°), which is lower than that of graphene oxide (9.55°). This could imply that the interplanar spacing of GO functioned with DAB was broadened due to possible intercalation of DAB, and that GO was fully exfoliated by treatment with DAB. Therefore, the XRD patterns confirm also the formation of DAB grafting on the surfaces of GO [28]. On the other hand, the GO peak disappears in the XRD pattern of GODABE (Fig. 3c), and other new characteristic peaks can be seen, these new bands corresponding to the chemically converted the functionalization graphene oxide into GOBABE, and at the same time indicating that GO sheet is uniformly an interaction with EDTA without agglomeration.

Adsorption of BB Dye onto GO, GODAB, and GODABE

The batch system was employed in adsorption experiments of CR dye onto prepared adsorbents at optimum pH, contact time, and temperature.

Effect of pH

The pH of the dye solution assumes a significant role in the whole adsorption experiment, particularly on the adsorption capacity. The pH solutions can affect the surface charge of the adsorbent and the degree of the ionization of different pollutants [29]. The effect of pH on the BB dye adsorption capacities onto GO, GODAB, and GODBE were studied at 400.0 mg/L initial dye concentration and fixed adsorbent dosage 25.0 mg for 45 min. Figure 4, illustrates the pH influence of the adsorption capacities at different pH values ranging from 3.0 to 12.0 at 27°C. As shown in Fig. 4, the adsorption capacity of BB dye decrease with increasing the pH of solution from 3.0 for adsorbents GO and GODAB, where the maximum adsorption recorded as highest values in pH 3.0 compared the pH range from 6.0 to 12.0. The q_{max} values were 708.42 mg/g for GO, 1322.1 mg/g for GODAB at pH 3.0, and 600.87 mg/g at pH 5.0 for GODABE that increase as pH values increase from 3.0 to 5.0. Notably, that the surface of all adsorbents contains different functional groups such as carboxylic and amine groups, the change in pH of dye solution will effect on the ionization of these functional groups [30,31]

Effects of agitation time and temperature on the adsorption

The duration time before the adsorption process reaches equilibrium called agitation time [32], Fig. 5 (a, b and c) shows the plots for the effect of agitation time on the adsorption of BB dye at pH 3.0 onto adsorbents GO, GODAB and 5.0 onto GODABE at different temperatures. Seemingly, from Fig. 5a, the adsorption of BB rapidly increased from (1-45 min), then the equilibrium was attained within (45-60 min) for adsorbent GO. While for adsorbents GODAB and GODABE (Fig. 5b and c) the increasing was rapidly from (1-30 min), then equilibrium was attained within (30-60 min). Also, the adsorption capacity for all adsorbents GO, GODAB, and GODABE increased as temperature rising from 27°C to 60°C. Since the adsorption processes for

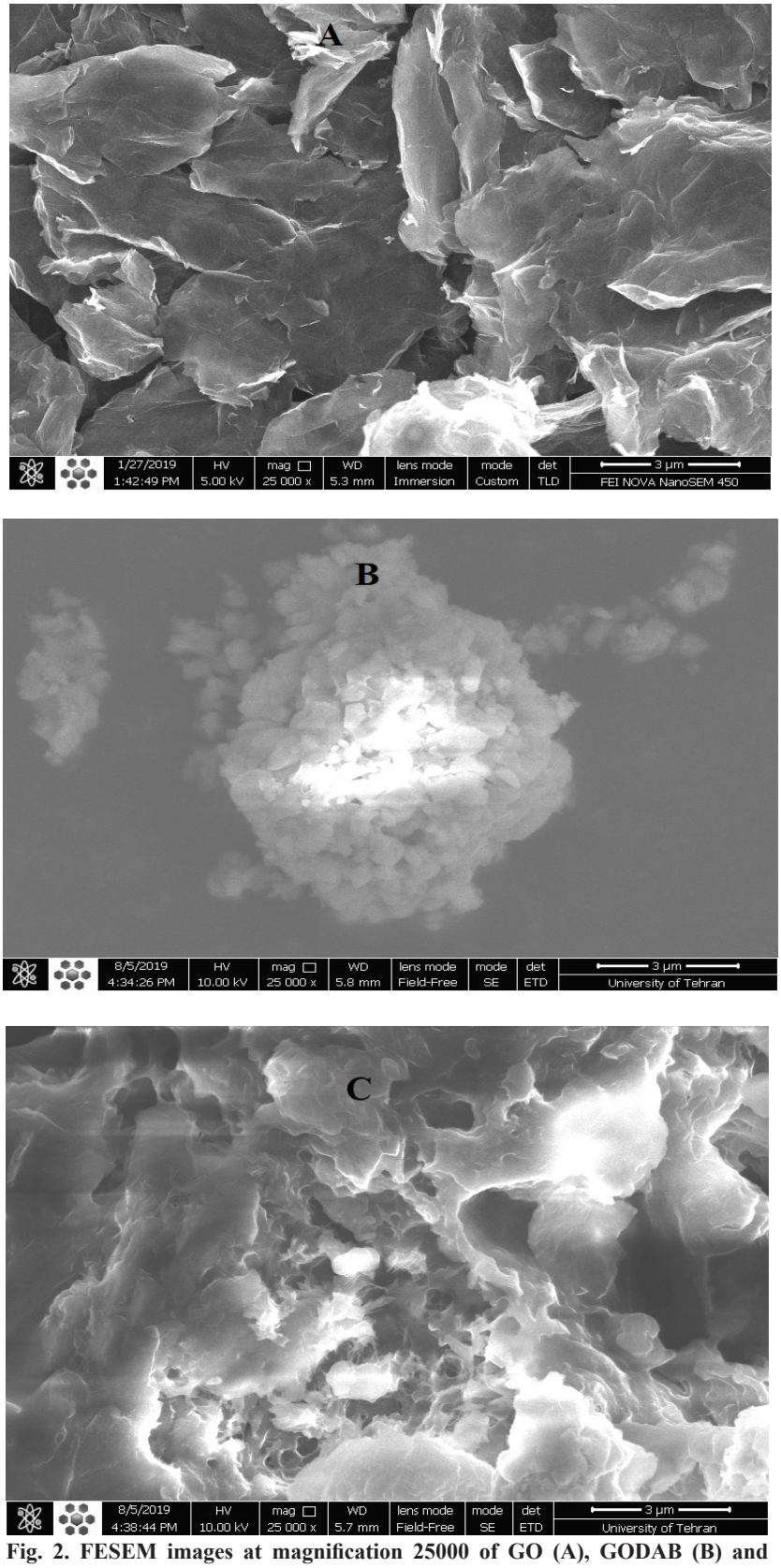

Fig. 2. FESEM images at magnification 25000 of GO (A), GODAB (B) and GODABE (C).

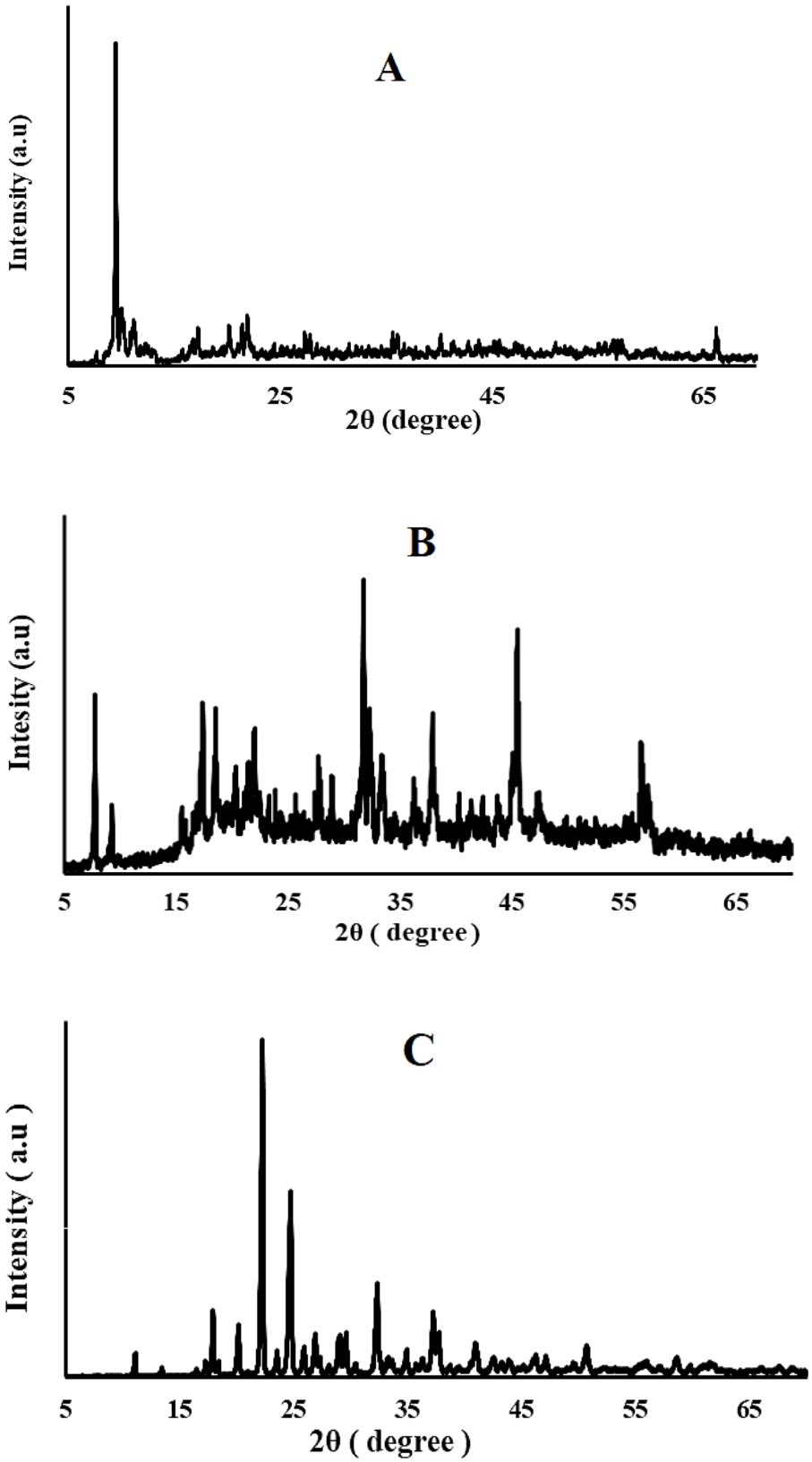

Fig. 3.XRD patterns of GO (A), GODAB (B), and GODAB (C).

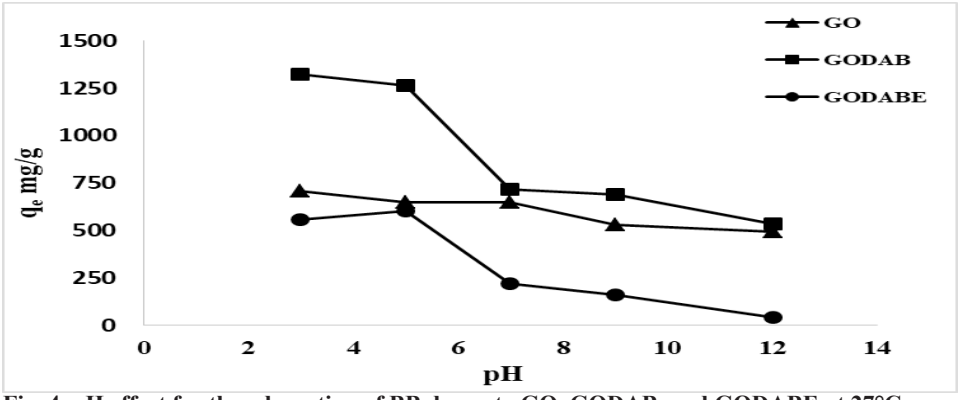

Fig. 4. pH effect for the adsorption of BB dye onto GO, GODAB, and GODABE at 27°C.

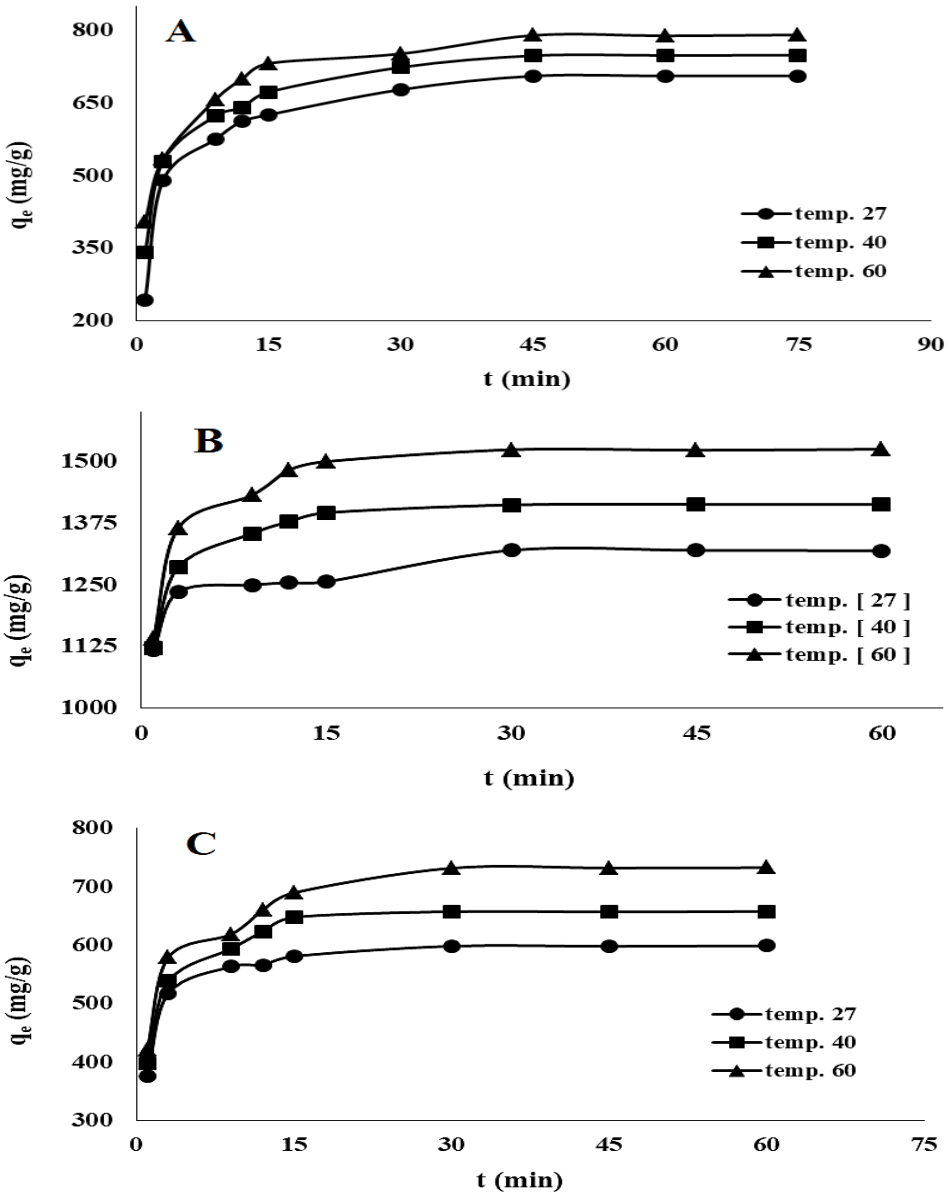

Fig. 5. Agitation time effect for the adsorption of BB dye onto (A) GO, (B) GODAB, and (C) GODABE at 27°C.

all adsorbents were endothermic. This tendency for adsorption capacities of these adsorbents is expected. Thus, the optimum agitation times for all further experiments were chosen as 45 min for adsorption of BB dye by adsorbent GO, and 30 min for both adsorbents GODAB and GODABE.

Adsorption isotherms studies

The adsorption isotherm appears distribution of molecules between solid and liquid phases at equilibrium state. The isotherm data analysis of fitting the data to different isotherm models is an essential step in finding the most reasonable model that can be used to explain the adsorption process [33]. The Langmuir model depends upon the maximum adsorption that coincides with the saturated monolayer of adsorbate molecules on the adsorbent surface. When plotting C_e/q_e versus C_e, the slope of a plot equal to $(1/q_{max})$ and intercept equal to $(1/q_{max} . K_L)$, and Fig. 6 shows the plots of Langmuir adsorption isotherms of BB dye adsorbed onto GO, GODAB, and GODABE respectively. Freundlich isotherm is based on a heterogeneous exponentially decaying distribution, which fits well with the tailing portion of the heterogeneous distribution of adsorbent [34]. Fig.7 exhibits the plots of Freundlich adsorption isotherms of BB dye onto GO, GODAB, and GODABE which determined from the linear plot of lnq_e versus lnC_e. The values of the Langmuir and Freundlich isotherm parameters and the

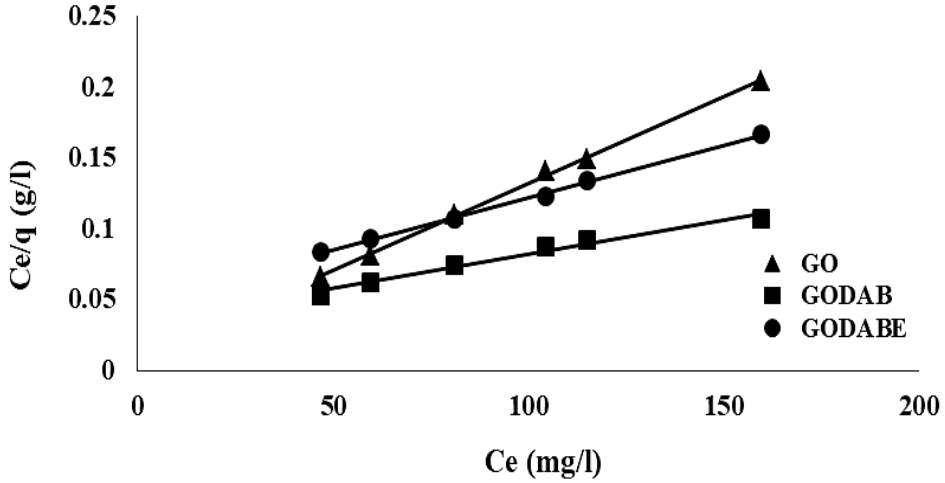

Fig. 6. Langmuir adsorption isotherm of BB dye onto GO, GODAB, and GODABE at 27°C.

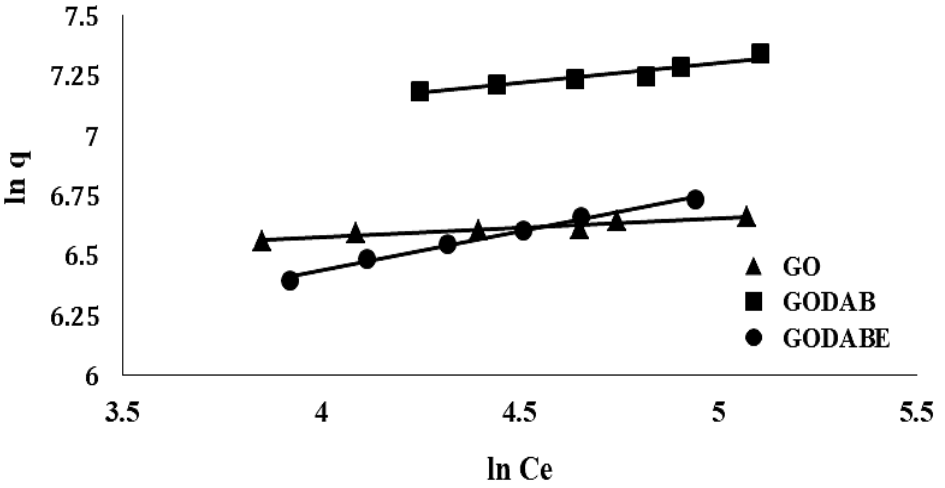

Fig. 7. Freundlich adsorption isotherm of BB dye onto GO, GODAB, and GODABE at 27°C.

TABLE 1. Langmuir and Freundlich isotherm parameters for adsorption of BB Dye onto Adsorbents at 27°C.

Adsorbent	q_{max}	Langmuir isotherm			Freundlich isotherm		
		K_L	R_L	R^2	K_F	1/n	R^2
GO	833.3	0.12632	0.01941	0.9988	527.158	0.0772	0.9004
GODAB	1666.6	0.0425	0.05549	0.9929	642.329	0.1676	0.9273
GODABE	1111.1	0.02387	0.09480	0.9993	169.051	0.3268	0.9907

correlation coefficient R^2 are given in Table 1. It demonstrates the linearity of the Langmuir isotherm equation was more fitting with comparing that isotherm equation of Freundlich and indicated normal Langmuir isotherm behaviors of dye adsorption onto adsorbents.

Kinetics studies

Three kinetic models were tested to explain the adsorption mechanism of BB dye onto GO, GODAB, and GODABE. The first model was pseudo-first-order, the mathematical expression of this model given by Eq. 6. Plotting of 1/ q_t versus 1/t gives the rate constants K_1 and correlation coefficient R^2. Fig. 8 (A, B, and C) shows the pseudo-first-order equations for BB dye at different temperatures.

The second kinetic model was pseudo-second-order, which represented by the Eq. 7. Values of q_2 and K_2 were calculated from the plot of t/q_t versus t from the slope and intercept, respectively (Fig. 9 A, B, and C).

Intra-particle diffusion was the last model tested in this study; the equation of the intra-particle diffusion model is given by Eq. 8. Fig. 10 (A, b, and C) displays the intra-particle diffusion equations for BB dye at different temperatures. The kinetic data for the adsorption of BB dye onto GO, GODAB, and GODABE at different temperatures were calculated from related plots and are summarized in Table 2. The obtained R^2 values from pseudo-first-order and pseudo-second-order adsorption models are $\leq$0.980 and $\geq$0.999, respectively. Moreover, the calculated values of q match highly effective with the experimental data. This suggests that the kinetic modelling of the temperature effect on the adsorption process is more likely to fit the models of the pseudo-second-order adsorption [35].

Thermodynamic study

The enthalpy, entropy and the free energy changes for BB dye adsorption onto GO, GODAB, and GODABE were calculated as per the equilibrium data, and their values are shown in Table 3. At all studied temperatures, the negative values of $\Delta G°$ indicate that the adsorption process is spontaneous, reflecting the affinity of adsorbents towards the cationic dye. The positive value of $\Delta H°$ confirms the endothermic nature of the adsorption. The positive value of $\Delta S°$ for the adsorption of BB dye onto all adsorbents explains the increase of the adsorption process randomness and affinity of the adsorbents for BB dye. Low activation energy E_a <40 kJ/mol are characteristics of the physisorption mechanism and diffusion-controlled process.

Desorption studies

Desorption studies are important to elucidate the reusability of an adsorbent and to understand the nature of adsorption system and evaluate the ability of recycling, and Table 4 shows the desorption percentages of the three-cycle were (40.00, 73.50, and 69.36%) for BB onto GO, GODAB, and GODABE respectively, that is mean that these adsorbents could be used several times while retaining its good adsorption capacity.

Conclusions

In our study, graphene oxide GO, GODAB, and GODABE that synthesized based on graphite powder and investigated to evaluate the removing applicability of BB dye from the aqueous solutions. The maximum adsorption of BB was obtained at pH (3.0) for GO, GODAB, and pH (5.0) for GODABE, also the adsorption system in this study increased with temperature increasing for all adsorbents, and fitted the Langmuir model, concluded that the operations of adsorption might be chemical behavior. From the linearized Langmuir equation, q_{max} values were (833.3, 1666.7, and 1111.1 mg/g) for GO, GODAB, and GODABE respectively. Depending on the valued of the correlation coefficient R^2, the pseudo-second-order kinetic model accurately described the adsorption kinetics

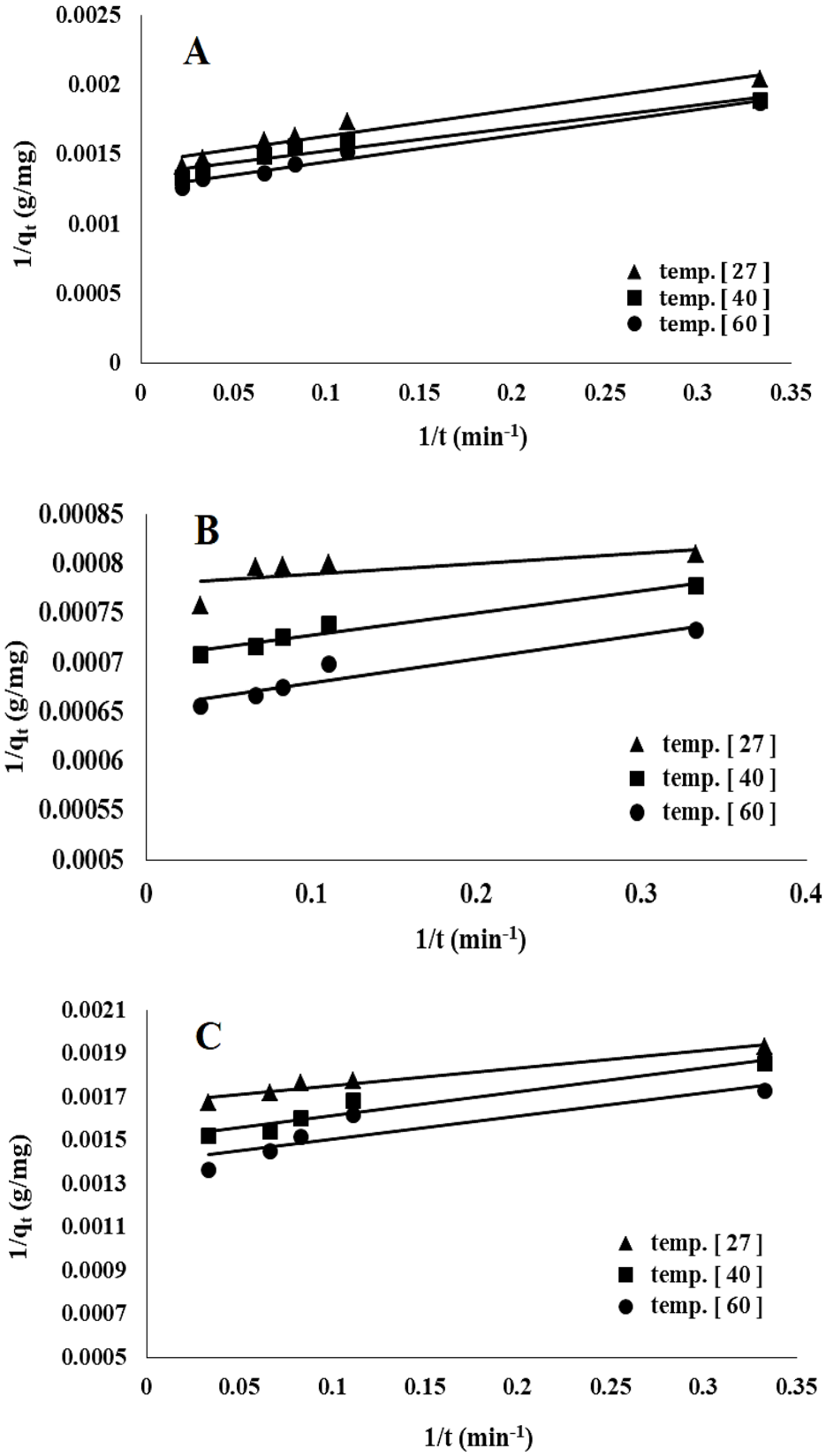

Fig. 8. Pseudo-First-Order plots for the adsorption of BB dye onto (A) GO, (B) GODAB, and (C) GODABE at 27, 40, and 60°C.

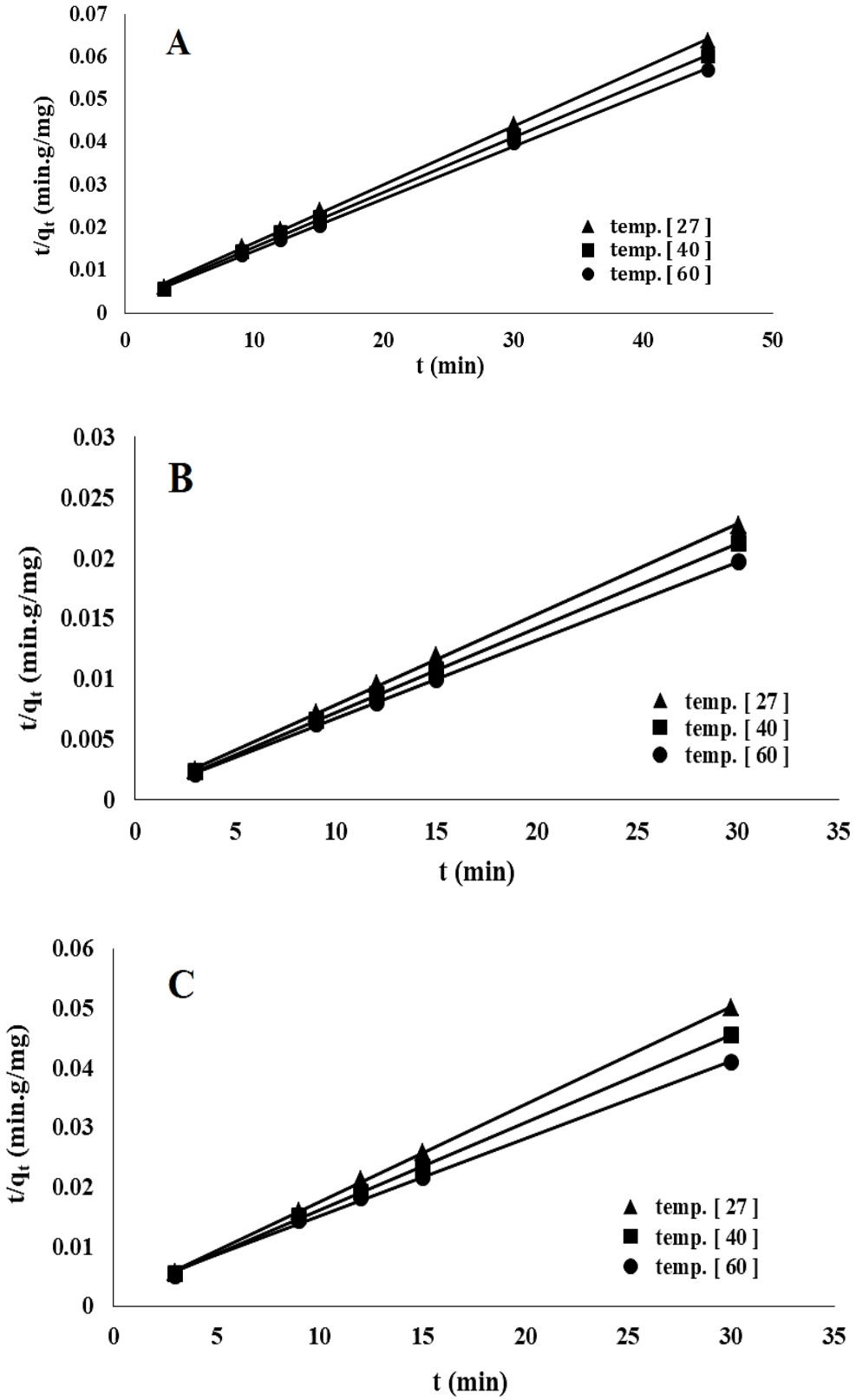

Fig. 9: Pseudo-Second-Order plots for the adsorption of BB dye onto (A) GO, (B) GODAB, and (C) GODABE at 27, 40, and 60°C.

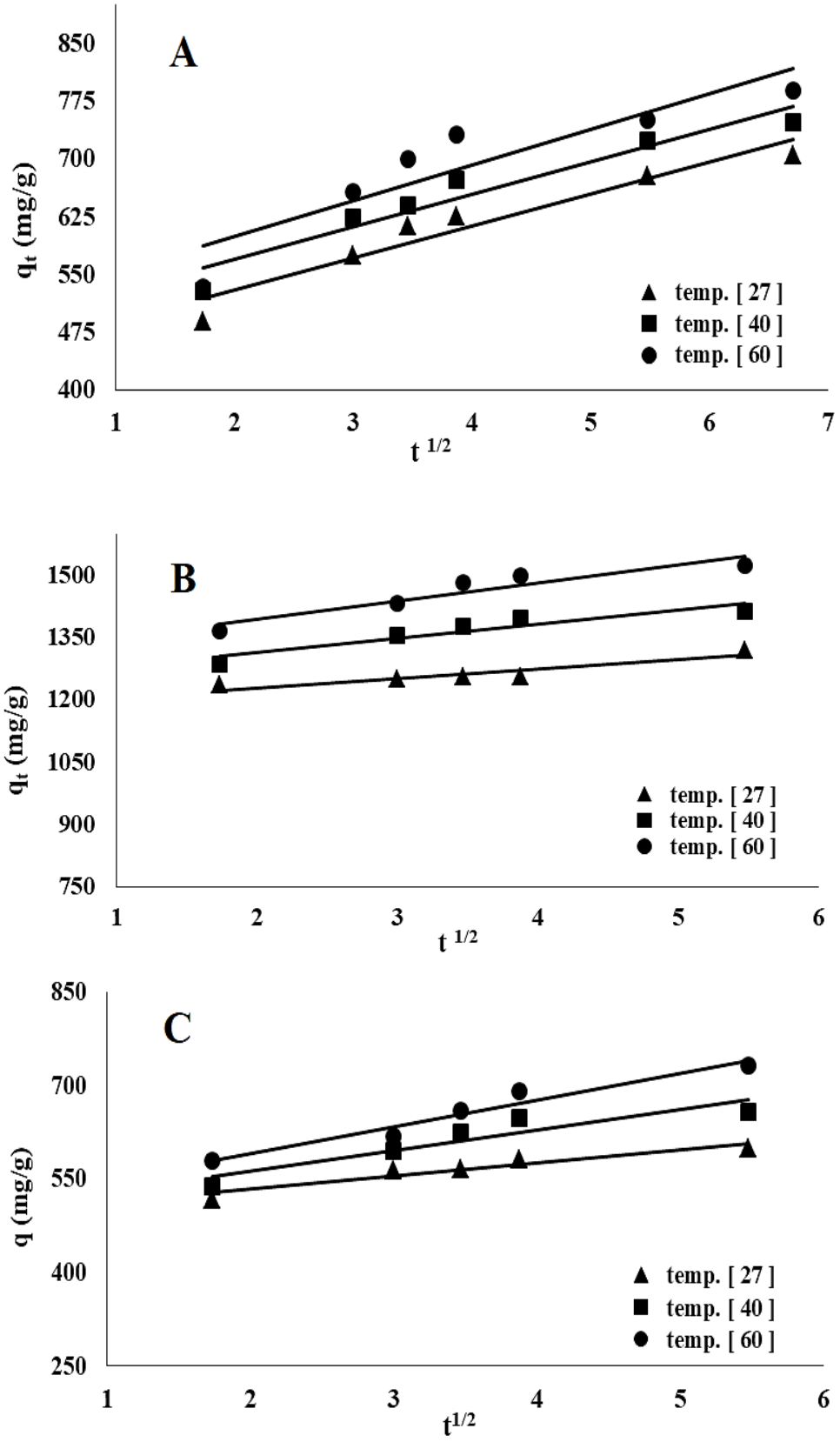

Fig. 10. Intra-particle diffusion plots for the adsorption of BB dye onto (A) GO, (B) GODAB, and (C) GODABE at 27, 40, and 60°C.

TABLE 2. Kinetic parameters for adsorption of BB dye onto adsorbents at constant pH and different temperatures.

Adsorbents	Temp. (°C)	Psedo-first-order			Psedo-second-order			Intra-particle diffusion		
		K_1	q_1	R_1^2	K_2	q_2	R_2^2	K_p	C	R_p^2
GO	27	1.35	714.28	0.938	0.00065	714.28	0.9992	42.492	437.12	0.943
	40	1.21	714.28	0.932	0.00063	769.23	0.9993	44.027	468.99	0.9645
	60	1.46	769.50	0.980	0.00060	833.33	0.9993	47.118	491.50	0.9076
GOCS	27	0.12	1250	0.420	0.00123	1428.5	0.9992	22.347	1184.6	0.8588
	40	0.28	1428.2	0.961	0.00163	1428.5	1	33.560	1247.4	0.8621
	60	0.02	142.85	0.906	0.00280	1666.6	0.9999	43.440	1308.4	0.8741
GOpBCM	27	0.47	588.23	0.954	0.00213	625	0.9998	22.347	491.23	0.9112
	40	0.73	666.66	0.932	0.00161	666.66	0.9995	33.560	498.05	0.8552
	60	0.78	714.28	0.796	0.0004	769.23	0.9979	43.441	505.93	0.9526

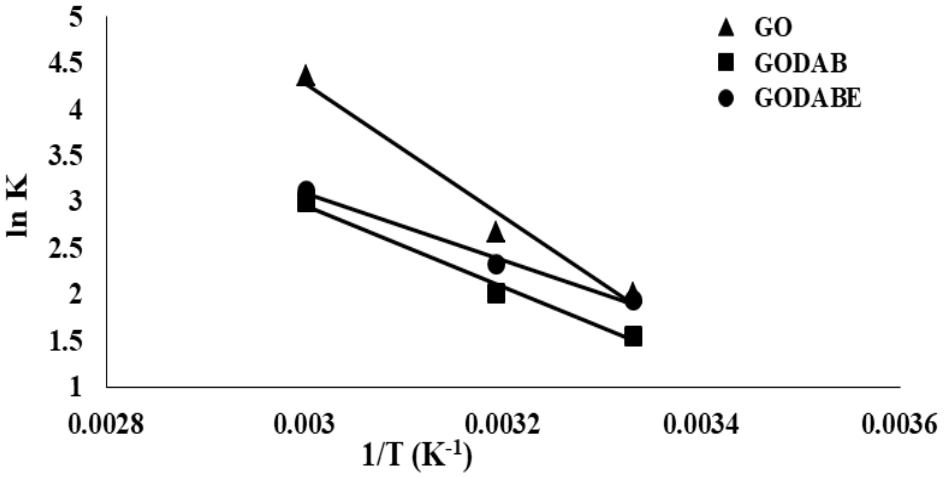

Fig. 11. Thermodynamic parameters for the adsorption of BB dye onto GO, GODAB, and GODABE.

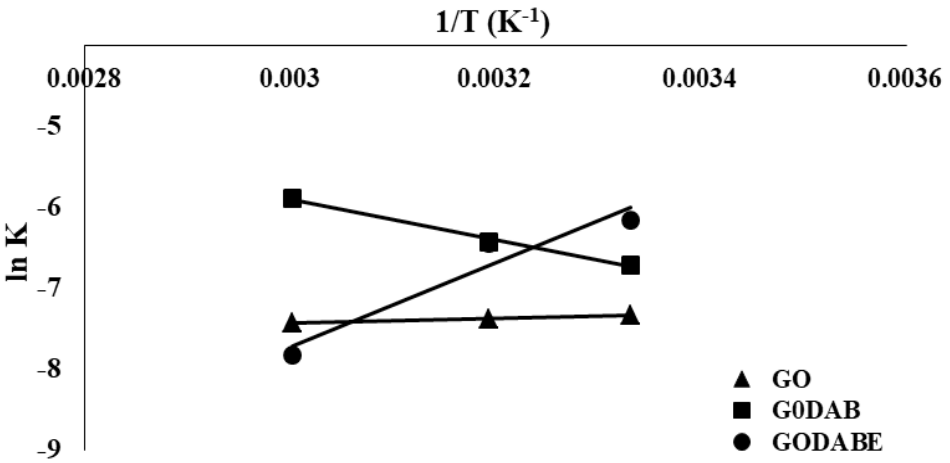

Fig. 12. Activation energy for the adsorption of BB dye onto GO, GODAB, and GODABE.

TABLE 3. Thermodynamic parameters for adsorption of BB dye onto adsorbents at different temperatures.

Adsorbent	Temp.	ΔH°	ΔS°	- ΔG°	E_a
GO	300.15	60.175	216.172	4.7091	2.126
	313.15			7.5193	
	333.15			11.843	
GODAB	300.15	36.856	216.172	28.028	20.973
	313.15			30.838	
	333.15			35.162	
GODABE	300.15	29.954	115.565	4.732	43.310
	313.15			6.234	
	333.15			8.545	

TABLE 4. Adsorption/Desorption for CR dye onto adsorbents.

Cycle No.	GO		GODAB		GODABE	
	q_e	%S	q_e	%S	q_e	%S
1	714.28	60.30	1428.50	81.40	1111.10	76.20
2	387.31	46.05	1231.04	77.00	940.10	72.32
3	303.06	40.00	1139.00	73.50	900.090	69.36

for BB dye onto adsorbents. Thermodynamic parameters showed that the nature of adsorption systems of the adsorbents was physisorption; thus, the adsorption processes could be said to have chemical and physical nature.

References

1. Nippatla, N.; Philip, L., Electrocoagulation-floatation assisted pulsed power plasma technology for the complete mineralization of potentially toxic dyes and real textile wastewater. Process Safety and Environmental Protection **125,** 143-156 (2019),.
2. Manimekalai, T.; Tamilarasan, G.; Sivakumar, N.; Periyasamy, S., Kinetic, equilibrium and thermodynamic studies of synthetic dye removal using plastic waste activated carbon prepared by CO_2 activation. International Journal of ChemTech Research, 8 (6), 225-240 (2015).
3. Wijannarong, S.; Aroonsrimorakot, S.; Thavipoke, P.; Sangjan, S., Removal of reactive dyes from textile dyeing industrial effluent by ozonation process. APCBEE procedia, 5, 279-282. (2013).
4. Pavithra, K. G.; Kumar, S.; Jaikumar, V., Removal of colorants from wastewater: A review on sources and treatment strategies. Journal of Industrial and Engineering Chemistry, 75, 1-19 (2019) .
5. Somasundaram, S.; Veerakumar, P.; Lin, K. C.; Kumaravel, V., Application of Nanocomposites for Photocatalytic Removal of Dye Contaminants. Photocatalytic Functional Materials for Environmental Remediation, 131-161 (2019).
6. Dhingra, N.; Singh, N. S.; Parween, T.; Sharma, R., Heavy Metal Remediation by Natural Adsorbents. In Modern Age Waste Water Problems, Springer: ; pp 233-250 (2020).
7. Wu, S.; Li, Z.; Sarma, H. K., Influence of confinement effect on recovery mechanisms of CO2-enhanced tight-oil recovery process considering critical properties shift, capillarity and adsorption. Fuel, 262, 116569 (2020).
8. Jeon, C.; Höll, W. H., Chemical modification of chitosan and equilibrium study for mercury ion removal. Water Research, 37 (19), 4770-4780 (2003).
9. Xing, H. T.; Chen, J. H.; Sun, X.; Huang, Y. H.;

Su, Z. B.; Hu, S. R.; Weng, W.; Li, S. X.; Guo, H. X.; Wu, W. B., NH2-rich polymer/graphene oxide use as a novel adsorbent for removal of Cu (II) from aqueous solution. Chemical Engineering Journal, 263, 280-289 (2015).

10. Stankovich, S.; Dikin, D. A.; Piner, R. D.; Kohlhaas, K. A.; Kleinhammes, A.; Jia, Y.; Wu, Y.; Nguyen, S. T.; Ruoff, R. S., Synthesis of graphene-based nanosheets via chemical reduction of exfoliated graphite oxide. carbon, 45 (7), 1558-1565 (2007).

11. Bertsias, G. K.; Tektonidou, M.; Amoura, Z.; Aringer, M.; Bajema, I.; Berden, J. H.; Boletis, J.; Cervera, R.; Dörner, T.; Doria, A., Joint European League Against Rheumatism and European Renal Association–European Dialysis and Transplant Association (EULAR/ERA-EDTA) recommendations for the management of adult and paediatric lupus nephritis. Annals of the rheumatic diseases, 71 (11), 1771-1782 (2012).

12. Repo, E.; Warchoł, J. K.; Bhatnagar, A.; Sillanpää, M., Heavy metals adsorption by novel EDTA-modified chitosan–silica hybrid materials. Journal of colloid and interface science, 358 (1), 261-267 (2011).

13. White, R. L.; White, C. M.; Turgut, H.; Massoud, A.; Tian, Z. R., Comparative studies on copper adsorption by graphene oxide and functionalized graphene oxide nanoparticles. Journal of the Taiwan Institute of Chemical Engineers, 85, 18-28 (2018).

14. Ghorbani, M.; Shams, A.; Seyedin, O.; Lahoori, N. A., Magnetic ethylene diamine-functionalized graphene oxide as novel sorbent for removal of lead and cadmium ions from wastewater samples. Environmental Science and Pollution Research, 25 (6), 5655-5667 (2018) .

15. Cui, L.; Wang, Y.; Gao, L.; Hu, L.; Yan, L.; Wei, Q.; Du, B., EDTA functionalized magnetic graphene oxide for removal of Pb (II), Hg (II) and Cu (II) in water treatment: Adsorption mechanism and separation property. Chemical engineering journal, 281, 1-10 (2015).

16. Zafara, S.; Khanb, M. I.; Khraishehd, M.; Hussain, M.; Mirzab, M. L.; Khalidi, N., Kinetic, equilibrium and thermodynamic studies for adsorption of nickel ions onto husk of Oryza sativa. DESALINATION AND WATER TREATMENT, 167, 277-290 (2019).

17. Khan, M. I.; Zafar, S.; Buzdar, A. R.; Azhar, M. F.; Hassan, W.; Aziz, A., Use Of Citrus Sinensis Leaves As A Bioadsorbent For Removal Of Congo Red Dye From Aqueous Solution. FEB-Fresenius Environmental Bulletin, 4679 (2018).

18. Allam, O.; Fathy, N.; Khafagj, M.; El-Bisi, M., Modified Waste Materials for Removal of Cationic Dye from Liquid Effluents and Their Kinetic Studies. EGYPTIAN JOURNAL OF CHEMISTRY, 58 (2), 141-154 (2015) .

19. Zhong, M.; Liu, Y.-T.; Xie, X.-M., Self-healable, super tough graphene oxide–poly (acrylic acid) nanocomposite hydrogels facilitated by dual cross-linking effects through dynamic ionic interactions. Journal of Materials Chemistry B, 3 (19), 4001-4008 (2015).

20. Ma, J.; Cai, P.; Qi, W.; Kong, D.; Wang, H., The layer-by-layer assembly of polyelectrolyte functionalized graphene sheets: a potential tool for biosensing. Colloids and Surfaces A: Physicochemical and Engineering Aspects, 426, 6-11 (2013).

21. Shan, R.-r.; Yan, L.-g.; Yang, K.; Yu, S.-j.; Hao, Y.-f.; Yu, H.-q.; Du, B., Magnetic Fe3O4/MgAl-LDH composite for effective removal of three red dyes from aqueous solution. Chemical Engineering Journal, 252, 38-46 (2014).

22. Extremera, R.; Pavlovic, I.; Pérez, M.; Barriga, C., Removal of acid orange 10 by calcined Mg/Al layered double hydroxides from water and recovery of the adsorbed dye. Chemical engineering journal, 213, 392-400 (2012) .

23. Cui, L.; Guo, X.; Wei, Q.; Wang, Y.; Gao, L.; Yan, L.; Yan, T.; Du, B., Removal of mercury and methylene blue from aqueous solution by xanthate functionalized magnetic graphene oxide: sorption kinetic and uptake mechanism. Journal of colloid and interface science, 439, 112-120 (2015).

24. Zhao, C.; Ma, L.; You, J.; Qu, F.; Priestley, R. D., EDTA-and amine-functionalized graphene oxide as sorbents for Ni (II) removal. Desalination and Water Treatment, 57 (19), 8942-8951 (2016).

25. Ma, H.-L.; Zhang, Y.; Hu, Q.-H.; Yan, D.; Yu, Z.-Z.; Zhai, M., Chemical reduction and removal of Cr (VI) from acidic aqueous solution by ethylenediamine-reduced graphene oxide. Journal of Materials Chemistry, 22 (13), 5914-5916 (2012).

26. Liu, G.; Wang, L.; Wang, B.; Gao, T.; Wang, D., A reduced graphene oxide modified metallic cobalt composite with superior electrochemical performance for supercapacitors. RSC Advances, 5 (78), 63553-63560 (2015).

27. Blanton, T. N.; Majumdar, D., Characterization of X-ray irradiated graphene oxide coatings using X-ray diffraction, X-ray photoelectron spectroscopy, and atomic force microscopy. Powder Diffraction, 28 (2), 68-71 (2013).

28. Abd, A. N.; Al-Agha, A. H.; Alheety, M. A., Addition of Some Primary and Secondary Amines to Graphene Oxide, and Studying Their Effect on Increasing its Electrical Properties. Baghdad Science Journal, 13, 1 (2016).

29. Boumediene, M.; Benaïssa, H.; George, B.; Molina, S.; Merlin, A., Effects of pH and ionic strength on methylene blue removal from synthetic aqueous solutions by sorption onto orange peel and desorption study. J. Mater. Environ. Sci, 9, 1700-1711 (2018).

30. Shirmardi, M.; Mesdaghinia, A.; Mahvi, A. H.; Nasseri, S.; Nabizadeh, R., Kinetics and equilibrium studies on adsorption of acid red 18 (Azo-Dye) using multiwall carbon nanotubes (MWCNTs) from aqueous solution. Journal of Chemistry, 9 (4), 2371-2383 (2012).

31. Bazrafshan, E.; Mostafapour, F. K.; Hosseini, A. R.; Raksh Khorshid, A.; Mahvi, A. H., Decolorisation of reactive red 120 dye by using single-walled carbon nanotubes in aqueous solutions. Journal of chemistry, 2013 (2012)

32. Ngah, W. W.; Fatinathan, S., Chitosan flakes and chitosan–GLA beads for adsorption of p-nitrophenol in aqueous solution. Colloids and Surfaces A: Physicochemical and Engineering Aspects, 277 (1-3), 214-222 (2006).

33. Royer, B.; Cardoso, N. F.; Lima, E. C.; Vaghetti, J. C.; Simon, N. M.; Calvete, T.; Veses, R. C., Applications of Brazilian pine-fruit shell in natural and carbonized forms as adsorbents to removal of methylene blue from aqueous solutions—Kinetic and equilibrium study. Journal of Hazardous Materials, 164 (2-3), 1213-1222 (2009).

34. Xia, Y.-q.; Guo, T.-y.; Song, M.-d.; Zhang, B.-h.; Zhang, B.-l., Adsorption dynamics and thermodynamics of Hb on the Hb-imprinted polymer beads. Reactive and Functional Polymers, 68 (1), 63-69 (2008).

35. Ibrahim, A.; El Fawal, G. F.; Akl, M. A., Methylene Blue and Crystal Violet Dyes Removal (As A Binary System) from Aqueous Solution Using Local Soil Clay: Kinetics Study and Equilibrium Isotherms. Egyptian Journal of Chemistry, 62 (3), 541-554 (2019).

التوظيف الكيميائي لأوكسيد الجرافين لدراسة سلوك امتزاز صبغة بسمارك البنية من المحاليل المائية

علاء عادل مزهر[١]، علي عبدالرزاق عبدالواحد[٢] و هادي سلمان اللامي[٢]
[١]قسم علوم البحار التطبيقية - كلية علوم البحار- جامعة البصرة - العراق
[٢]قسم الكيمياء – كلية العلوم – جامعة البصرة - العراق

حضر في هذه الدراسة أوكسيد الكرافين ومشتقين أخرين من خلال مفاعلته مع كل من ٣,٣′–ثنائي أمينوبينزيدين على التوالي، GODABE و GODAB ومن ثم ثنائي أمين الإيثيلين رباعي حامض الأسيتيك لتكوين كل من وتم تشخيص المركبات المحضرة بواسطة الأشعة تحت الحمراء، الميكروسكوب الأليكتروني الماسح وكذلك حيود بواسطة المركبات المحضرة وكفاءة Bismarck Brown BB الاشعة السينية. أجريت دراسة امتزاز لصبغة امتزاز نفس الصبغة من قبل أوكسيد الكرافين لغرض المقارنة من خلال أعتماد نظام الوجبة في دراسة الأمتزاز ودرست آيزوثيرمات الآمتزاز لكل من لانجمير و فريندليتش، ووجد أن موديل لانجمير هو الأكثر تطابقاً وحسبت GODABE للمركب mg/g و ١١١١,١ GODAB للمركب mg/g وكانت تساوي ١٤٢٨,٥ q_{max} منها . كما درست حركية وثرموديناميكية الآمتزاز mg/gله تساوي ٧١٤,٢٨ q_{max} بالمقارنة مع أوكسيد الكرافين للصبغة ووجد ان تفاعلات الآمتزاز هي من النوع الباعث للحرارة وكذلك تلقائية، كما درست عملية أعادة أستخدام .المركبات المحضرة في عملية آمتزاز متتالية ووجد بأنه يمكن أعادة أستخدامها لثلاث دورات آمتزاز متتالية